Bioresource Technology Reports 34 (2026) 102644

Contents lists available at ScienceDirect

Bioresource Technology Reports

journal homepage: www.sciencedirect.com/journal/bioresource-technology-reports

Enhancing vibrational energy absorption in banana stem fibers through π–π stacking of curcumin on lignocellulose and structural reorganization by microwave irradiation

Hastawati Chrisna Suroso [a,b], Eko Siswanto [a], Sugiono [c], I.N.G. Wardana [a,*]

[a] Department of Mechanical Engineering, Brawijaya University, Jl. MT. Haryono 167, Malang, 65145, Indonesia
[b] Department of Industrial Engineering, Adhi Tama Surabaya Institute of Technology, Jl. Arief Rahman Hakim 100, Surabaya, 60117, Indonesia
[c] Department of Industrial Engineering, Brawijaya University, Jl. MT. Haryono 167, Malang, 65145, Indonesia

ARTICLE INFO

Keywords:
Lignocellulosic biomass
Banana stem fiber
Curcumin treatment
Microwave irradiation
π–π stacking
Damping performance

ABSTRACT

Lignocellulosic biomass is a promising renewable platform for high value functional materials. This study presents a bio-based modification strategy to enhance the vibrational energy absorption performance of banana stem fiber through curcumin immersion followed by microwave induced structural reorganization. Curcumin initially forms disordered π–π stacking interactions with the lignocellulosic, while microwave irradiation promotes their reorientation into a more ordered structure. This reorganization enhances intermolecular electron mobility and improves vibrational energy dissipation. Curcumin treated fiber shows the highest damping ratio with ζ approximately 0.049 ± 0.006, but with elevated RMS acceleration. Microwave treatment reduces RMS acceleration to 0.087 ± 0.008 m/s^2, which is nearly an order of magnitude lower and well below ISO 2631 comfort thresholds. The combined process converts low value biowaste into a high-performance damping material using a low energy and scalable approach, demonstrating its potential as a sustainable alternative to synthetic vibration isolation materials.

1. Introduction

Lignocellulosic biomass continues to gain prominence as a sustainable resource for developing high value functional materials, particularly as global industries transition toward greener and more circular material strategies (Tu and Hallett, 2019). Beyond its well-established role in biorefinery and bioenergy pathways, lignocellulosic biomass offers structural and functional attributes that can be engineered for broader applications, including damping, acoustic insulation, packaging, and composite reinforcement. In vibration sensitive systems such as transportation platforms, agricultural machinery, industrial equipment, and human machine interfaces, prolonged exposure to mechanical vibration contributes to structural degradation, operator discomfort, and long-term physiological strain as defined under ISO 2631 standards (Zhao and Schindler, 2014). These concerns have intensified research interest in biodegradable vibration attenuating materials as alternatives to synthetic polymers, which often exhibit poor environmental compatibility and limited end of life recyclability.

Among natural fiber candidates, banana stem fiber emerges as an abundant bio waste material with favorable characteristics. Prior studies have demonstrated its low density, high specific strength, favorable stiffness to weight ratio, and inherent capacity for energy dissipation under cyclic loading (Ali et al., 2022; Gupta et al., 2020).These characteristics make banana stem fiber suitable for vibration reduction in components such as seating structures, floor panels, support modules, and vibration isolation layers. However, despite its advantages, untreated lignocellulosic fiber exhibits intrinsic molecular level limitations. These limitations include irregular aromatic stacking, restricted electron delocalization, a porous and heterogeneous microstructure, and a high concentration of hydroxyl groups that increase moisture uptake and reduce intermolecular cohesion (Gupta et al., 2020). As a result, the native fiber structure lacks molecular stability under dynamic vibrational conditions, which diminishes its ability to absorb energy effectively.

A growing body of research has explored the use of microwave energy to modify the physical and chemical structure of lignocellulosic

* Corresponding author.
E-mail addresses: chrisnasuroso@student.ub.ac.id (H.C. Suroso), eko_s112@ub.ac.id (E. Siswanto), sugiono_ub@ub.ac.id (Sugiono), wardana@ub.ac.id (I.N.G. Wardana).

https://doi.org/10.1016/j.biteb.2026.102644
Received 9 December 2025; Received in revised form 13 February 2026; Accepted 13 February 2026
Available online 18 February 2026

biomass. (Ethaib, 2024) highlighted the novelty of microwave pretreatment in reducing activation energy, enhancing interfacial transport, and improving substrate digestibility, with performance strongly dependent on parameters such as exposure time, power level, and moisture content. While valuable, these studies remain oriented toward biorefinery applications and do not examine how microwave-induced structural changes could be employed to reorganize aromatic domains, enhance molecular cohesion, or improve mechanical properties relevant to damping performance (Romero-Zúñiga et al., 2023).

At the molecular scale, research by (Kustanto et al., 2024) revealed that microwave induction can reorganize π–π stacking arrangements and increase charge mobility within RGO curcumin C60 hybrid systems through changes in effective activation energy and compression ratio. This work demonstrates the ability of microwave fields to influence electronic interactions and aromatic stacking. However, these findings are limited to engineered graphene-based systems and have not yet been extended to natural lignocellulosic fibers. Moreover, the existing body of work remains focused on thermal conversion applications and does not explore the use of curcumin as a molecular modifier for enhancing vibrational damping in biomass-derived materials. Notably, very few researchers have considered leveraging enhanced electron mobility through π–π stacking interactions as a mechanism for dissipating mechanical vibration energy in such systems.

In this context, the present study examines how a curcumin-rich turmeric extract is dominated by curcumin and related curcuminoids will introduces aromatic π-conjugated domains capable of forming hydrogen bonds with cellulose, hemicellulose, and lignin (Li et al., 2021). Curcumin is regarded as the principal active species within the extract and provides the π-stacking potential and hydrogen-bonding functionality that influence molecular association within the fiber network.

The aromatic nature of curcumin facilitates microstructural alignment, moderates hydroxyl-related polarity, and promotes localized densification within the fiber matrix—factors that contribute to enhanced viscoelastic behavior and structural stability (Li et al., 2021; Moghaddam et al., 2021). Nevertheless, curcumin treatment alone does not fully address the limitations associated with disordered aromatic domains or insufficient molecular ordering, indicating the need for a complementary activation method to achieve more coherent structural organization.

Microwave irradiation provides a complementary mechanism for enhancing these effects. Through dielectric heating, microwave energy facilitates molecular chain mobility, promotes localized structural reorganization, and increases the alignment of aromatic domains. Prior studies also indicate that microwave exposure can enhance surface roughness, reduce moisture affinity, and improve internal fiber morphology. However, the combined interaction between curcumin treatment and microwave irradiation in lignocellulosic fibers has not been systematically investigated. Understanding this interaction is essential for developing high performance bio based damping materials.

In this context, the present study investigates the synergistic effects of curcumin treatment and microwave irradiation on the structural, chemical, and vibrational performance of banana stem fiber. Three configurations are evaluated: untreated fiber, curcumin treated fiber, and curcumin treated fiber subjected to microwave irradiation. Vibrational performance is assessed through RMS acceleration, damping ratio, and tan delta measurements referenced to ISO 2631, enabling evaluation of material suitability for vibration sensitive environments. Microstructural and chemical modifications are characterized using FTIR, FESEM EDS, XRD with Rietveld refinement, and thermogravimetric analysis (Guruguntla and Lal, 2022; de la Hoz-Torres et al., 2022). This work proposes a new biomass valorization pathway in which curcumin induced π–π stacking is reorganized under microwave activation to produce a high-performance bio-based damping material. The findings offer a scalable, energy efficient, and environmentally compatible strategy for transforming bio waste into functional materials suitable for engineering applications where vibration control is critical.

2. Materials and methods

2.1. Fiber extraction

Banana pseudo stem trunks (*Musa* spp., family *Musaceae*), predominantly derived from commonly cultivated local banana plants such as *Musa acuminata* and related cultivars, were obtained from local plantations in East Java, Indonesia, and used as the primary lignocellulosic material. The trunks were mechanically processed using a decorticator machine without chemical additives. The extracted fibers were washed thoroughly with clean water to remove sap residues and surface impurities, then sun dried to reduce moisture content to ambient levels. The resulting fibers ranged from approximately 120 to 200 cm in length.

2.2. Curcumin treatment and material preparation

Raw banana pseudo stem fibers, composed primarily of cellulose, hemicellulose, and lignin, were cut into 20-cm segments prior to treatment. Based on Van Soest compositional analysis, the raw banana stem fiber used in this study exhibited 84.34% neutral detergent fiber (NDF) and 64.30% acid detergent fiber (ADF), corresponding to average contents of 20.05% hemicellulose, 12.38% cellulose, and 52.39% lignin. A curcumin-rich turmeric extract (CRTE) was obtained by mechanically pressing fresh *Curcuma longa* rhizomes using a slow juicer. This process generated a natural extract containing curcuminoids (primarily curcumin, demethoxycurcumin, and bisdemethoxycurcumin), volatile oils, and aqueous components released from the rhizome matrix, without added solvents or chemical reagents. Based on the maceration-based extraction process employed and the resulting extract characteristics, the primary curcumin content in the liquid turmeric extract can be reasonably estimated to be on the order of tens of micrograms per milliliter. In the present study, the curcumin concentration is estimated to be approximately 35.2 μg/mL, corresponding to 3.52 mg per 100 mL of extract. The overall experimental workflow, sample configurations, and vibration testing arrangement are illustrated in Fig. 1.

A total of 120 g of fiber was prepared for each batch and immersed in 500 mL of freshly pressed curcumin-rich turmeric extract (CRTE), maintaining a consistent fiber-to-extract ratio. Preliminary trials showed that volumes below 500 mL led to incomplete submersion and visibly uneven wetting along the fiber length, with some portions remaining exposed to air. This condition, referred to as non-uniform uptake, reflects heterogeneous surface contact rather than a quantified absorption parameter. Using 500 mL ensured full submersion and more homogeneous solution diffusion throughout the fiber network, consistent with immersion-based biomass modification methods (Thimmegowda et al., 2025). After immersion, the fibers were drained and sun dried to remove residual surface moisture.

2.3. Microwave irradiation

Microwave modification was conducted using a domestic microwave oven (Electrolux; nominal output power 900 W; operating frequency 2.45 GHz; power supply 220 V, 50 Hz). Fiber samples were placed on a rotating glass turntable at the center of the microwave cavity to promote uniform exposure to the electromagnetic field. Irradiation was performed at medium power for a total duration of 120 s, with the total fiber mass per batch maintained at 120 g.

During microwave irradiation, the surface temperature of the fiber samples was monitored using an infrared thermometer immediately after exposure. The temperature increased from 27.6 ± 0.35 °C at 0 s to 40.5 ± 0.54 °C at 30 s, 50.0 ± 0.63 °C at 60 s, 51.1 ± 0.53 °C at 90 s, and reached approximately 52.5 ± 0.55 °C after 120 s. This temperature profile indicates a rapid initial heating stage followed by a plateau, suggesting limited bulk thermal accumulation during prolonged

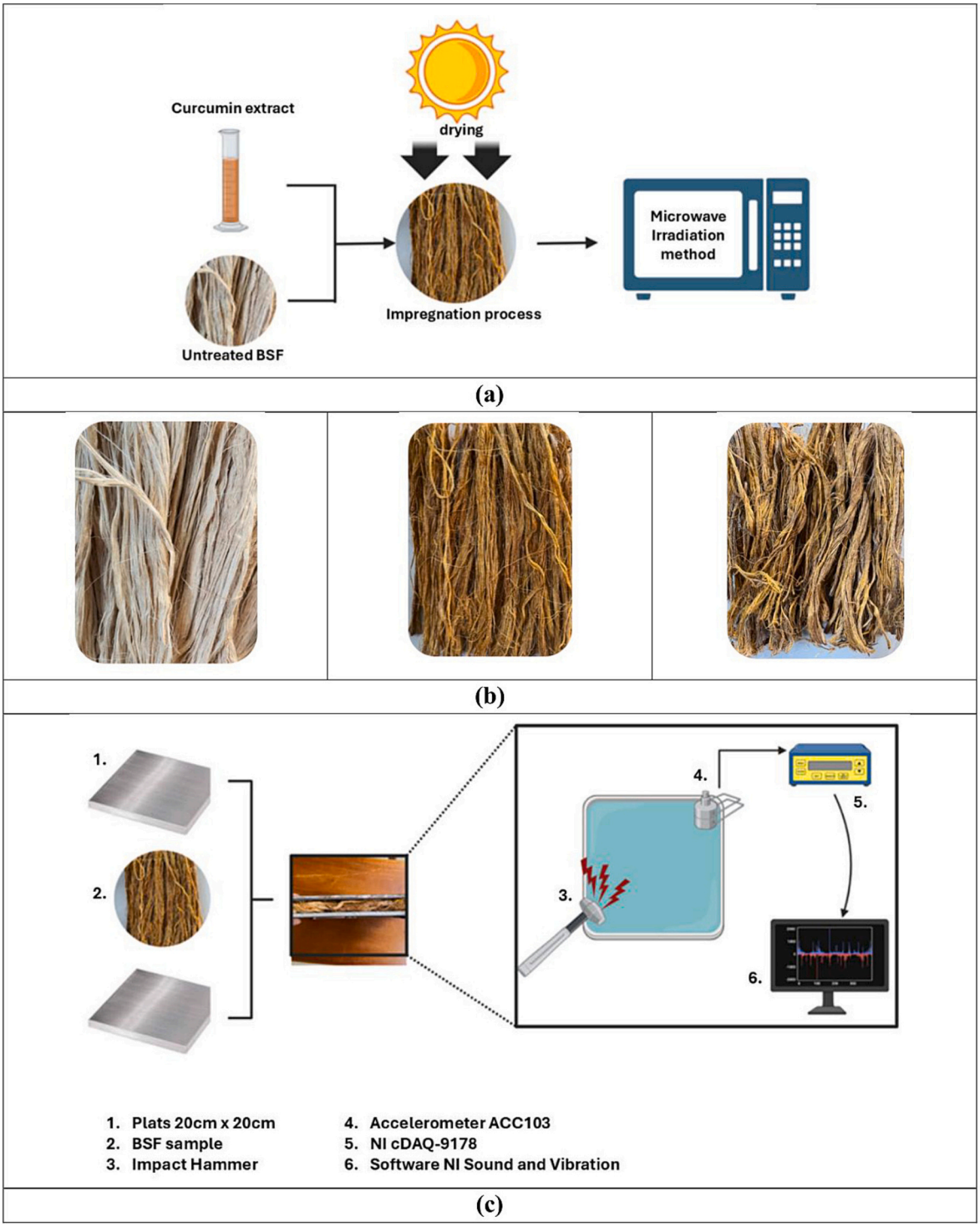

Fig. 1. Experimental workflow and sample configuration: (a) Fiber extraction & curcumin immersion (b) Sample variants (BSF, BSF + Curcumin, BSF + Curcumin+Microwave) (c) Vibration test setup.

irradiation.

Previous studies on microwave-assisted modification of lignocellulosic fibers have commonly employed activation times up to 90 s (Kustanto et al., 2024). In the present work, preliminary trials at 60 and 90 s resulted in insufficient microstructural modification and limited improvement in damping response. Accordingly, the irradiation duration was extended to 120 s to promote enhanced molecular mobility and interfacial interaction between curcumin and the fiber matrix under microwave dielectric heating conditions. Prior to irradiation, the fibers were fully dried to minimize moisture-related variability and to ensure more consistent microwave energy coupling.

2.4. Experimental setup for vibration testing

The vibration testing arrangement is illustrated in Fig. 1(c). Treated and untreated fiber samples were placed between two iron plates (20 cm by 20 cm), each weighing 120 g. An accelerometer was attached to the upper plate and connected to an NI Sound and Vibration data acquisition

system to record transient acceleration responses. The opposite edge of the plate was exciting using a light impact hammer suitable for modal excitation (B and K 202). The plate fiber plate assembly was positioned on a rigid support to ensure consistent boundary conditions during impact excitation.

A sampling rate of 10 kHz was used for vibration data acquisition. Acceleration time histories were collected and converted into attenuation curves. The vibration parameters were calculated using standard vibration analysis procedures.

2.5. Material characterization

Structural and chemical analysis of untreated, curcumin treated, and curcumin microwave treated fibers was performed using the following techniques:

2.5.1. FTIR

Fourier Transform Infrared (FTIR) spectroscopy was performed using a Shimadzu IRSpirit-T spectrometer equipped with an attenuated total reflectance (ATR) accessory (IRSpirit/ATR-S). Spectra were collected over a spectral range of 4000–500 cm^{-1} with a resolution of 4 cm^{-1} and averaged over 10 scans per sample. The Happ–Genzel apodization function was applied during spectral acquisition. All spectra are presented in percent transmittance (%T).

2.5.2. XRD

Crystallographic analysis was carried out using a PANalytical X'PERT 3 Powder diffractometer equipped with Cu Kα radiation ($\lambda = 1.5406$ Å) operating at 40 kV and 30 mA. Scans were recorded from 10 to 90 degrees with a step size of 0.0167 degrees. Rietveld refinement was performed using Profex software.

2.5.3. FESEM and EDS

Morphological analysis was performed using a Quanta FEG650 Field Emission Scanning Electron Microscope. Elemental composition was assessed using an Oxford X Act Energy Dispersive X ray Spectroscopy detector.

2.5.4. TGA

Thermogravimetric analysis was performed using a Shimadzu DTG 60 instrument from 30 to 800 degrees Celsius under a nitrogen atmosphere to evaluate thermal stability, moisture release, and degradation behavior of the fibers.

2.5.5. Polarization resistance measurement

Polarization measurements were conducted to evaluate the interfacial charge transport behavior of untreated and modified BSF samples. The measurements were performed using an Autolab PGSTAT204 potentiostat controlled by NOVA software. Linear sweep voltammetry (LSV) was applied in staircase mode, with a potential range from −0.500 V to +0.500 V, a step potential of 0.00500 V, and a scan rate of 0.0050000 V/s. Polarization resistance values were extracted from the resulting polarization curves and used as semi-quantitative indicators of charge transfer resistance and interfacial polarization behavior.

3. Result and discussion

3.1. Surface morphology observed through FESEM

Surface morphology plays a pivotal role in governing the interfacial behavior and energy dissipation mechanisms in natural fiber-based damping systems. Understanding morphological transitions induced by surface modifications is therefore essential to improve the performance of bio-based vibration isolators.

Field Emission Scanning Electron Microscopy (FESEM) revealed a progressive transformation in the surface morphology of banana stem fiber (BSF) across untreated, curcumin-treated, and microwave-activated conditions (Fig. 2a–c). The untreated fiber (Fig. 2a) exhibited a relatively smooth and continuous surface with longitudinal fibrillar lines, which are characteristic of natural banana fibers. Only minor superficial particles and occasional depressions were observed, suggesting a compact and unmodified lignocellulosic structure with limited surface reactivity. These features are consistent with previous findings describing the inherently low interfacial activity of untreated natural fibers (Zhang and He, 2022).

In contrast, curcumin-treated BSF (Fig. 2b) displayed significant surface roughening, along with the emergence of microchannels and heterogeneous porosity. These modifications are attributed to curcumin adsorption via hydrogen bonding and aromatic interactions at the fiber surface. The phenolic and methoxy functional groups of curcumin partially disrupted the native microfibrillar arrangement, resulting in a reoriented surface topology. This reorganization is expected to enhance π–π stacking potential and improve interfacial compatibility under mechanical excitation (Mansingh et al., 2022). Such morphological alterations support improved interfacial friction and more efficient stress redistribution during vibrational loading.

Subsequent microwave treatment (Fig. 2c) further intensified these surface changes. Dielectric heating induced localized molecular motion that led to the partial collapse of microvoids, reduction of hydroxyl groups, and densification of the surface, while preserving the overall fiber integrity. Residual hydroxyl regions appeared to serve as anchoring points for curcumin, facilitating its dispersion and attachment across the fiber surface. These effects collectively promoted nanoscale structural rearrangement and better molecular alignment, consistent with reports on microwave-assisted modification of natural fibers (Barros et al., 2024; Hidalgo-Salazar et al., 2024; Ponce-Ruiz et al., 2022).

It is important to distinguish these microwave-induced morphological changes from those reported under ultrasound-based treatments. Prior work has shown that prolonged ultrasonic irradiation results in limited cellulose disruption, with surface changes confined largely to superficial fibrillation and minor roughness (Yu et al., 2025). In contrast, the current study shows more pronounced nanoscale restructuring, suggesting that microwave irradiation provides additional molecular-level driving forces, such as dipolar polarization and localized dielectric heating. These mechanisms enable hydrogen-bond rearrangement and promote greater interaction between the curcumin aromatic domains and the reorganized cellulose matrix.

The observed morphological evolution supports existing evidence that untreated BSF exhibits low surface reactivity (Zhang and He, 2022), whereas curcumin introduces functional aromatic regions that promote hydrogen bonding and interfacial compatibility (Drouiche et al., 2023). The present findings further confirm that curcumin enhances both the surface texture and energy dissipation capacity of BSF, consistent with previous reports (Almutairi et al., 2021).

Compared to curcumin treatment alone, the combination of microwave and curcumin modification produced a more extensive nanoscale restructuring. Similar trends in enhanced crystallinity, surface activation, and fibrillar alignment under microwave conditions have been observed in other lignocellulosic systems such as bamboo and kenaf fibers (Barros et al., 2024; Hidalgo-Salazar et al., 2024). The interaction between curcumin and the reorganized cellulose matrix appears to strike a balance between reduced hydroxyl content and enhanced aromatic conjugation, both of which contribute to improved stiffness and damping response.

In summary, FESEM analysis demonstrates that microwave assisted curcumin treatment reorganizes the cellulose microstructure, enhances surface heterogeneity, strengthens π–π conjugation, and promotes localized densification. These factors collectively increase electron mobility and interfacial energy dissipation, supporting the improved damping performance observed in later sections. The enhanced curcumin attachment and more uniform nanoscale features confirm the effectiveness of this dual treatment approach in producing a structurally

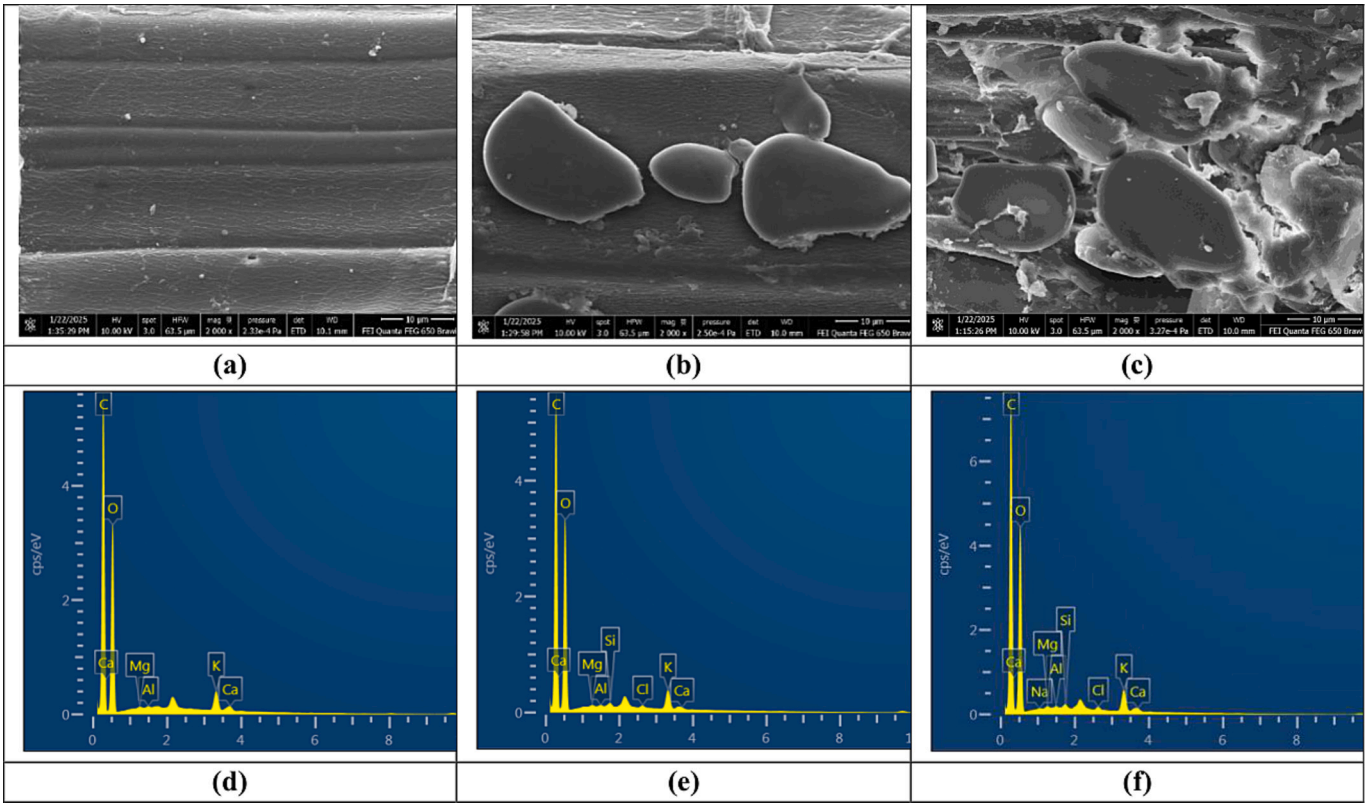

Fig. 2. FESEM images and SEM–EDS spectra of banana stem fiber (BSF) under different treatments: (a, d) untreated, (b, e) after curcumin treatment, and (c, f) after curcumin–microwave activation. Surface morphology changes are evident with treatment, while EDS confirms a carbon–oxygen-dominated composition without foreign elemental contamination.

responsive and sustainable vibration damping material (Drouiche et al., 2023).

3.2. Elemental composition based on EDS analysis

Energy Dispersive X-ray Spectroscopy (EDS) was employed to investigate the elemental composition of banana stem fiber (BSF) before and after surface modification, as shown in Fig. 2d–f. The untreated BSF (Fig. 2d) presented prominent carbon and oxygen peaks, corresponding to the presence of cellulose, hemicellulose, and lignin. Trace levels of potassium, calcium, magnesium, and aluminium were also detected, consistent with natural inorganic residues embedded within the plant cell wall. The high oxygen content reflects the abundance of hydroxyl groups, which contribute to the hydrophilic nature and reduced structural compactness of unmodified natural fibers (Patty and Wattimena, 2023).

After curcumin treatment (Fig. 2e), a noticeable increase in carbon signal intensity was observed. This change corresponds to the aromatic-rich carbon structure of curcumin and serves as indirect evidence of its successful attachment to the fiber surface. Minor fluctuations in oxygen levels suggest localized alterations in bonding interactions between curcumin functional groups and the cellulose matrix. These results align with previous studies reporting that curcumin imparts additional aromatic domains and hydrogen bonding sites to lignocellulosic substrates, which can alter the surface chemistry and enhance molecular association (Smalley et al., 2024).

Microwave activation further modified the elemental distribution (Fig. 2f), resulting in the appearance of intensified signals for sodium, silicon, and chlorine. These changes imply a redistribution of ionic species within the fiber matrix, likely driven by microwave-induced dielectric heating. Localized dehydration and increased ionic mobility under microwave exposure can facilitate reorganization of hydrogen bonding networks, as documented in related studies on electromagnetic treatment of plant-based materials (Silva et al., 2023; Zhang et al., 2022). The persistence of major carbon and oxygen peaks confirms that the treatment does not degrade the primary organic framework of the fiber.

The EDS profile of untreated BSF corresponds to typical natural fiber compositions dominated by organic polymers and minor inorganic elements, where high oxygen levels indicate hydroxyl rich, moisture sensitive regions with limited crystalline order (Patty and Wattimena, 2023; Sakib et al., 2024). The elevated carbon content observed after curcumin treatment supports previous reports on curcumin's polyphenolic contribution to improved structural organization (Smalley et al., 2024). Furthermore, the microwave assisted elemental redistribution is consistent with literature describing enhanced microstructural uniformity and ionic adjustments under dielectric heating (Silva et al., 2023).

Overall, sequential curcumin treatment and microwave activation introduce a compositional shift characterized by increased carbon levels, ion redistribution, and improved elemental uniformity. These changes may support enhanced electron mobility, dielectric responsiveness, and energy dissipation during vibrational loading, reinforcing the potential of microwave assisted curcumin modification as a sustainable strategy for optimizing natural fiber damping performance.

3.3. Functional group changes from FTIR spectroscopy

Fourier Transform Infrared (FTIR) spectroscopy was used to evaluate the evolution of functional groups in banana stem fiber (BSF) subjected to curcumin treatment and microwave activation. Spectra were recorded under consistent ATR conditions to ensure reliable comparisons across samples. As shown in Fig. 3a–b, untreated BSF exhibited a broad OH stretching band near 3300 cm^{-1} with approximately 65% transmittance, characteristic of abundant hydroxyl groups present in

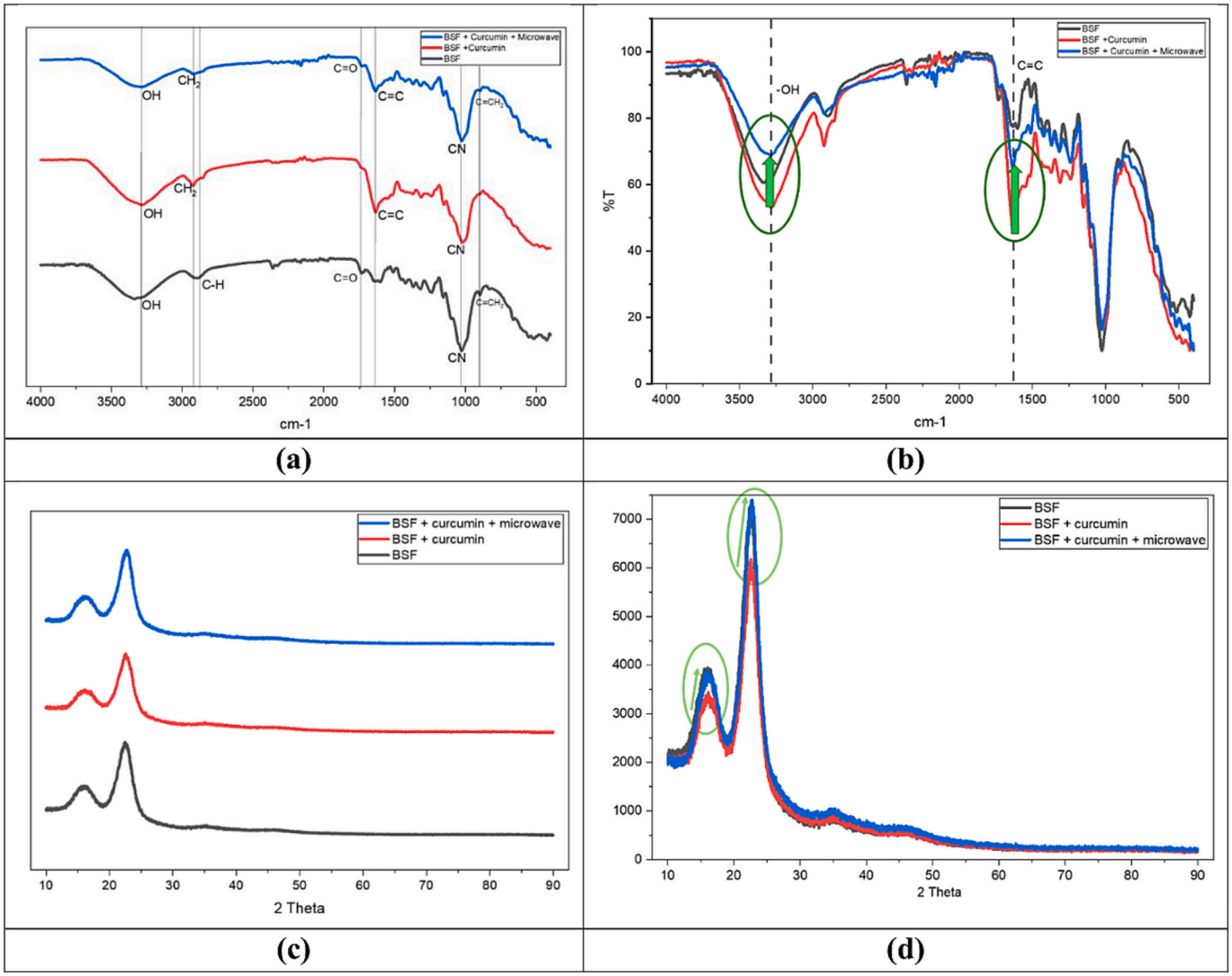

Fig. 3. Molecular and crystalline structural evolution of banana stem fiber induced by curcumin treatment and microwave activation:
(a) Representative FTIR spectra of untreated BSF, BSF + curcumin, and BSF + curcumin + microwave;
(b) FTIR transmittance (%T) comparison highlighting variations at characteristic hydroxyl and aromatic bands associated with molecular reorganization;
(c) XRD patterns plotted using normalized intensity to compare relative crystalline domain evolution;
(d) XRD patterns plotted using absolute intensity to emphasize changes in peak intensity and amorphous background contribution.
XRD measurements were conducted using Cu Kα radiation (λ = 1.5406 Å) over a 2θ range of 10–90°.

cellulose and hemicellulose. This absorption is indicative of a hydrophilic and largely amorphous lignocellulosic matrix (Xu et al., 2024).

Following curcumin incorporation, the OH band decreased in transmittance to approximately 50%, reflecting the formation of hydrogen bonds between curcumin's phenolic and carbonyl groups and the native hydroxyl sites in the fiber. This reduction suggests tighter molecular packing and increased interaction between the curcumin molecules and cellulose chains, which contributes to a more cohesive network. These observations are consistent with reports highlighting curcumin's strong affinity for lignocellulosic substrates and its ability to mediate interfacial bonding through aromatic and hydrogen bond interactions (Omoriyekomwan et al., 2022).

Microwave activation induced further spectral changes, most notably a rise in transmittance in the OH stretching region to around 75%, indicating a reduction in free hydroxyl content. This shift suggests partial dehydration and rearrangement of the hydrogen bonding network, in agreement with literature on microwave-induced structural consolidation in natural fibers (Dhanenderan et al., 2022). Additionally, a distinct aromatic C═C stretching band near 1633 cm^{-1} increased in intensity from ~45% transmittance after curcumin treatment to nearly 65% post-microwave activation. The growth of this band confirms the successful integration of curcumin and formation of more ordered aromatic structures.

These spectral developments correspond closely with literature describing the chemical modification of natural fibers. The pronounced OH absorption in untreated BSF is a hallmark of cellulose-based materials (Xu et al., 2024), while the emergence and intensification of aromatic C═C bands after treatment validate the formation of π–π stacking interactions and improved structural alignment resulting from curcumin incorporation (Omoriyekomwan et al., 2022). Curcumin's phenolic and carbonyl groups have been shown to promote stronger molecular association with cellulose, generating a more ordered arrangement and increased compatibility in functional materials.

The combination of microwave energy and curcumin promotes a transition toward greater rigidity and structural coherence within the fiber. Prior studies have shown that microwave processing facilitates crosslinking, reduces amorphous regions, and enhances crystalline domains in lignocellulosic materials ((Dhanenderan et al., 2022;

Omoriyekomwan et al., 2022), thereby improving structural organization. Such refinements are desirable for vibration damping applications, as enhanced charge transport and reduced moisture sensitivity contribute to improved long-term mechanical performance. Consistent with these observations, the FTIR results indicate that curcumin treatment coupled with microwave irradiation induces selective functional group reorganization and shifts the interaction mechanism from hydrogen-bond-dominated associations toward a more ordered aromatic network. This structural transformation enhances stability, lowers hydrophilicity, and potentially expands charge transport pathways, thereby reinforcing high-performance damping behavior.

Importantly, microwave treatment induced a controlled temperature increase from 27.6 ± 0.35 °C to 52.5 ± 0.55 °C; however, the maximum temperature remained well below the thermal degradation threshold of lignocellulosic constituents, indicating that structural modification occurred without thermal decomposition. Therefore, the observed spectral transformations are primarily attributed to dielectric effects, such as dipolar polarization and localized field-induced molecular motion, rather than simple thermal activation. This distinction underscores the specificity and effectiveness of microwave irradiation in engineering

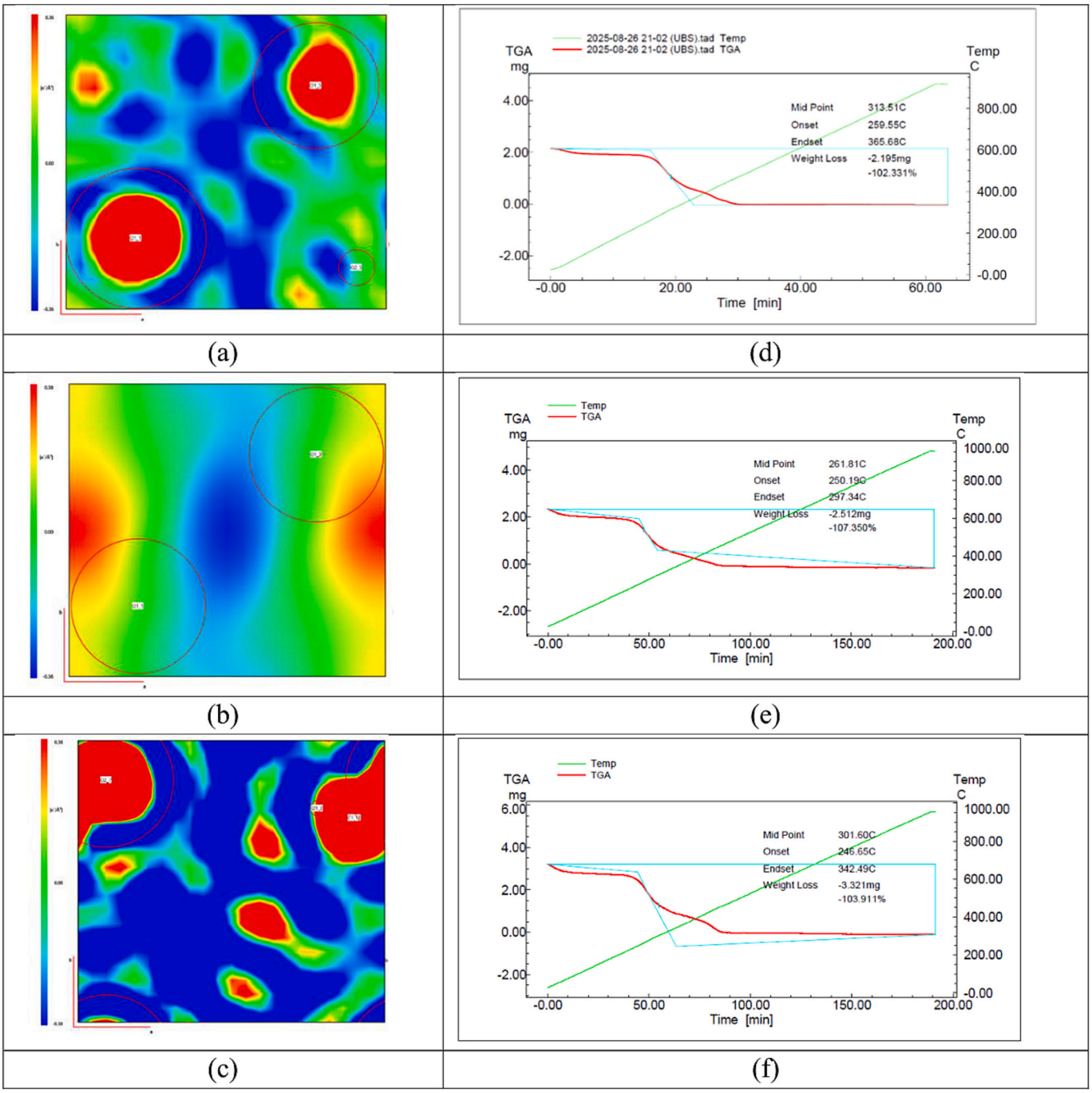

Fig. 4. Bulk structural reorganization and thermal response of banana stem fiber:
(a–c) Profex-based density maps illustrating relative internal structural reorganization for (a) untreated BSF, (b) BSF after curcumin treatment, and (c) BSF after combined curcumin and microwave activation, presented using identical color scales for direct comparison;
(d–f) TGA curves of (d) untreated BSF, (e) BSF + curcumin, and (f) BSF + curcumin + microwave, displayed in separate panels due to differences in thermal programs while maintaining consistent temperature and mass-loss scales.

functional modifications at the molecular level.

In conclusion, FTIR analysis confirms that curcumin treatment and microwave activation collaboratively reorganize the molecular structure of BSF. The resulting fiber displays a lower concentration of free hydroxyl groups, stronger aromatic domain alignment, and greater molecular cohesion. These features are advantageous for the development of natural fiber damping materials with enhanced interfacial performance, environmental stability, and suitability for vibration-sensitive engineering applications.

3.4. Structural ordering inferred from XRD and Profex visualization

X-ray diffraction (XRD) analysis was conducted to evaluate the crystalline structure of banana stem fiber (BSF) under untreated, curcumin-treated, and microwave-activated conditions. The diffraction patterns (Fig. 3c–d) revealed clear structural transitions corresponding to progressive molecular ordering within the cellulose matrix. Untreated BSF displayed broad peaks at $2\theta \approx 14^{\circ}$, 16°, and 22°, which are characteristic of cellulose I. The diffuse halo and relatively low peak intensities suggest a matrix dominated by amorphous hemicellulose and lignin, which hinder the development of crystalline domains (Zhan et al., 2023).

After curcumin incorporation, peak sharpness, particularly near the (002) plane at $2\theta \approx 22^{\circ}$, increased noticeably. This enhancement reflects improved molecular packing and localized ordering within the cellulose structure. The interaction of curcumin's aromatic and hydroxyl groups with cellulose chains has been shown to promote hydrogen bonding and partial crystallization, consistent with prior reports (Qian et al., 2022).

The most pronounced structural refinement was observed in the BSF treated with curcumin followed by microwave irradiation. This group exhibited the highest absolute diffraction intensity and the sharpest (002) peak at approximately $2\theta = 22.6^{\circ}$, alongside more distinct reflections at lower angles. These features indicate greater crystallinity, improved chain alignment, and reduced amorphous content. Microwave-induced dielectric heating is known to accelerate molecular mobility and promote structural reorganization in natural fibers, as documented in studies on bamboo and hybrid systems (Romero-Zúñiga et al., 2023; Sánchez-Martín et al., 2023).

Although crystallinity index values were not explicitly calculated, the enhanced sharpness and symmetry of the diffraction peaks across treatments qualitatively indicate improved molecular order. This structural development is relevant to vibration damping, as increased crystallinity typically contributes to enhanced stiffness and energy dissipation control (Barros et al., 2024; Hidalgo-Salazar et al., 2024).

Profex-based visualizations of the XRD data (Fig. 4a–c) provide complementary insight into internal ordering. The untreated fiber (Fig. 4a) shows a distribution dominated by blue to green regions, indicating low and heterogeneous electron density. These features are characteristic of amorphous cellulose microdomains and confirm the disordered internal architecture of the raw material (Wang et al., 2022).

In the curcumin-treated sample (Fig. 4b), the distribution transitions toward green to yellow regions, suggesting partial ordering and improved molecular interaction. This is consistent with curcumin's known ability to form hydrogen bonds and π–π interactions with cellulose, supporting semi-organized domains (Abdolmaleki et al., 2023).

The sample treated with both curcumin and microwave (Fig. 4c) reveals the most refined structure, with dense red regions indicating areas of elevated electron density. These zones are surrounded by well-defined gradients that delineate microstructural boundaries, which correspond to enhanced π–π stacking and lattice organization (Romero-Zúñiga et al., 2023). The sharp contrast across regions suggests the formation of well-aligned and densely packed domains, consistent with the intensified XRD reflections.

Although Profex is not a quantum-mechanical simulation tool, it can be effectively used to infer crystallographically consistent electron-density features from XRD data through Rietveld refinement followed by Fourier synthesis within the unit cell. In line with the Profex documentation and prior applications (Sobri et al., 2025), these maps are most appropriately interpreted in a relative sense and therefore should not be taken as absolute electron probability distributions. Accordingly, the red-highlighted regions are treated as qualitative indicators of locally higher relative electron density, which is compatible with increased aromatic-domain coherence and the strengthening of π–π stacking associated with curcumin-driven structural reorganization.

The integrated interpretation of XRD and Profex results provides a coherent understanding of the structural evolution of banana stem fibers induced by curcumin and further reinforced by microwave processing. Untreated BSF is predominantly characterized by amorphous, hydroxyl-rich regions with limited crystallinity, whereas the introduction of curcumin promotes local structural ordering through hydrogen bonding and aromatic interactions, as evidenced by sharper XRD reflections and a more homogeneous electron density distribution in the Profex maps. Subsequent microwave activation amplifies this reorganization by enhancing chain mobility, accelerating bound-water dehydration, and strengthening π–π stacking between the aromatic units of curcumin and cellulose microfibrils, thereby resulting in increased crystallinity and internal structural coherence. This sequential structural transformation underpins the improvements in mechanical and dielectric properties discussed in the following sections and highlights the effectiveness of the combined treatment strategy in optimizing fiber performance for vibration damping applications.

3.5. Thermal degradation behavior evaluated by TGA

Thermogravimetric analysis (TGA) was conducted to examine the thermal stability and degradation characteristics of banana stem fiber (BSF) under different surface treatments, as shown in Fig. 4d–f. The untreated BSF (Fig. 4d) exhibited the highest thermal resistance, with an initial degradation temperature of approximately 296 °C and a midpoint near 314 °C. These values reflect a dense hydrogen bonding network and a relatively ordered matrix of cellulose and hemicellulose, which are known to delay thermal decomposition in unmodified lignocellulosic materials (Schirp et al., 2024).

Curcumin-treated BSF (Fig. 4e) displayed a reduction in thermal stability, with the onset of degradation shifting to approximately 250 °C and the midpoint to around 262 °C. This decline is attributed to the presence of thermally labile aromatic and carbonyl groups introduced by curcumin, which undergo earlier breakdown. The increased total mass loss in this sample indicates a higher oxidative reactivity and reduced structural cohesion, likely caused by greater molecular free volume and less compact packing after curcumin incorporation (Singh et al., 2023).

Microwave activation following curcumin treatment (Fig. 4f) partially restored thermal stability. The onset temperature increased to about 265 °C, and the degradation midpoint rose significantly to approximately 302 °C. These improvements suggest that microwave exposure enhances molecular ordering and crosslinking through dielectric-driven dehydration and bond reorganization. This interpretation is supported by earlier FTIR and XRD results, which indicated reduced hydroxyl content and increased crystallinity in the microwave-treated fiber (Hasan et al., 2022; Schirp et al., 2024).

The thermal behavior of the untreated BSF aligns with established degradation pathways for natural fibers, where moisture evaporation is followed by hemicellulose and cellulose decomposition. The relatively high onset temperature indicates a tight hydrogen bonding structure and limited amorphous regions. This observation is consistent with the structural data discussed in the previous sections.

In the curcumin-treated sample, the lower degradation thresholds reflect the dual role of curcumin: while it enhances interfacial functionality, it also introduces molecular segments that are more susceptible to thermal breakdown. Curcumin's unsaturated domains can improve viscoelasticity while reducing thermal endurance (Singh et al.,

2023).

The microwave-treated curcumin sample demonstrated improved thermal resistance, which can be attributed to the increased chain alignment and densification of the cellulose matrix. These changes reduce the accessibility of oxygen and moisture, thereby delaying thermal decomposition. Prior studies have shown that microwave irradiation facilitates dehydration, promotes crystallinity, and reinforces covalent bonding in natural fiber structures (Hasan et al., 2022). The observed thermal enhancement is consistent with these mechanisms.

Overall, the TGA results confirm that microwave-assisted curcumin treatment leads to favorable thermal characteristics by balancing structural modification with improved cohesion. The upward shift in degradation temperatures indicates increased thermal robustness, which is advantageous for vibration damping applications exposed to fluctuating thermal and mechanical loads. These outcomes correlate with the improved damping performance and reduced RMS acceleration discussed in later sections.

3.6. Interfacial conductivity from polarization resistance

Polarization resistance provides a semi-quantitative insight into interfacial charge transport and polarization behavior within the modified BSF system, as commonly inferred from complex impedance responses in polarization-governed materials (Wang et al., 2025). As shown in Fig. 5a, the untreated fiber exhibits a relatively high polarization resistance of 319.73 Ω, indicating restricted charge displacement across poorly organized interfacial domains. Following curcumin incorporation, the resistance decreases substantially to 203.73 Ω and is further reduced to 188.26 Ω after combined curcumin treatment and microwave activation, reflecting progressively facilitated interfacial charge reorientation. Although polarization resistance does not directly quantify intrinsic electronic conductivity, the consistent reduction observed here suggests enhanced interfacial conductivity arising from improved structural coherence and aromatic-domain connectivity, in agreement with interphase-controlled polarization and charge-transfer behavior reported for lignin and cellulose-derwaived systems (Dong et al., 2025).

Under dynamic mechanical excitation, such interfacial modifications play a critical role in polarization-mediated energy dissipation. Increased charge mobility and polarizable interfacial regions respond to applied stress with a phase lag relative to mechanical deformation, thereby generating internal friction and dielectric loss. Consequently, a portion of the vibrational energy is converted into electrical polarization energy and subsequently dissipated as thermal energy through polarization resistance, contributing to enhanced damping performance. When interpreted in conjunction with FTIR and XRD analyses, which indicate strengthened aromatic interactions and reduced dominance of hydrogen-bonded amorphous regions, the polarization resistance results provide complementary support for a structure–property relationship linking interfacial reorganization to improved vibration attenuation. For clarity, charge mobility in this context is inferred from correlated electrical and structural trends rather than directly measured transport parameters.

3.7. Integrated assessment of damping, RMS, and stiffness

An integrated evaluation of damping behavior, stiffness, and vibration comfort reveals distinct functional trade-offs induced by curcumin incorporation and subsequent microwave activation. Dynamic vibration parameters, including logarithmic decrement, damping ratio, and RMS acceleration, were obtained from free vibration responses, as summarized in Table 1. Untreated BSF shows a low damping ratio of 0.004 ± 0.0007 with an RMS acceleration of 0.144 ± 0.010 m/s^2, indicating limited attenuation and reduced comfort performance. This baseline response is consistent with the amorphous-rich lignocellulosic architecture of natural fibers, where heterogeneous composition and limited structural coherence constrain energy dissipation and stability under dynamic excitation (Romero-Zúñiga et al., 2023), and it aligns with restricted interfacial charge reorientation inferred from earlier FTIR and Profex interpretations.

Curcumin treatment markedly enhances intrinsic damping, yielding the highest ζ and δ (ζ = 0.049 ± 0.006; δ = 0.308 ± 0.030). Aromatic and carbonyl functionalities introduce additional viscoelastic dissipation pathways and molecular friction during oscillatory deformation (Romero-Zúñiga et al., 2023). However, the highest RMS acceleration (0.877 ± 0.055 m/s^2) indicates greater instantaneous vibration transmission, suggesting that increased molecular mobility and compliance can amplify transient accelerations despite improved cycle-by-cycle dissipation. This interpretation is compatible with reduced thermal stability in TGA and increased flexibility associated with curcumin-rich domains (Singh et al., 2023).

Microwave activation shifts the response toward a more stable vibration regime by strongly suppressing RMS acceleration while maintaining moderate damping. The microwave-activated curcumin sample exhibits the lowest RMS acceleration (0.087 ± 0.008 m/s^2) and a reduced peak amplitude of approximately 0.254 m/s^2, indicating smoother transmission and improved comfort, while its damping ratio remains sufficient for gradual amplitude decay (ζ = 0.038 ± 0.005). This behavior is consistent with microwave-driven densification and enhanced molecular cohesion, where increased chain alignment and crystallinity improve resistance to peak vibrational loads and stabilize the dynamic response (Hasan et al., 2022). Strengthened π–π stacking and improved aromatic-domain coherence further support controlled, time-distributed dissipation rather than sharp acceleration spikes.

Stiffness provides a mechanistic basis for why RMS acceleration does not track damping ratio monotonically. Untreated BSF has a stiffness of 0.087 ± 0.020 N/mm, which increases to 0.131 ± 0.056 N/mm after curcumin treatment, accompanied by greater variability consistent with compliance and structural heterogeneity. After microwave activation, stiffness increases to 0.222 ± 0.100 N/mm, consistent with densification and improved molecular organization, thereby increasing dynamic load-bearing capability and suppressing peak accelerations. Consequently, a slightly lower damping ratio can still yield superior vibration comfort when stiffness-controlled dynamics reduce transient response.

From an application standpoint, the results indicate that damping ratio alone is insufficient for comfort-oriented vibration control, particularly in whole-body vibration contexts where RMS acceleration governs perceived severity. Accordingly, the microwave-activated curcumin-treated BSF provides the most practical balance between dissipation, stiffness-controlled dynamics, and comfort, whereas the curcumin-only system, despite maximal damping ratio, transmits higher instantaneous vibrations. The RMS values can be contextualized using ISO 2631 comfort considerations, and the relevant comfort zones are summarized in Table 2 (ISO 2631). To further establish practical relevance, the damping behavior is qualitatively benchmarked against representative natural fiber-based and synthetic vibration isolation materials, as presented in Table 3.

In addition to functional performance, the material system supports sustainability objectives because banana stem fibers are biodegradable and derived from agricultural residues. The use of food-grade curcumin and energy-efficient microwave processing avoids hazardous chemicals and petroleum-based additives. Although a full life cycle analysis is beyond the scope of this study, the treatment pathway demonstrates a feasible route toward green damping materials that couple structural performance with environmental responsibility.

Collectively, the integrated of damping, stiffness, and RMS assessment supports the conclusion that microwave-assisted curcumin treatment enables functional optimization rather than merely maximizing damping. By promoting cellulose architectural reorganization and improving interfacial coherence, the treatment strategy delivers controlled energy dissipation without compromising dynamic stability, consistent with the multi-technique structural evidence reported earlier

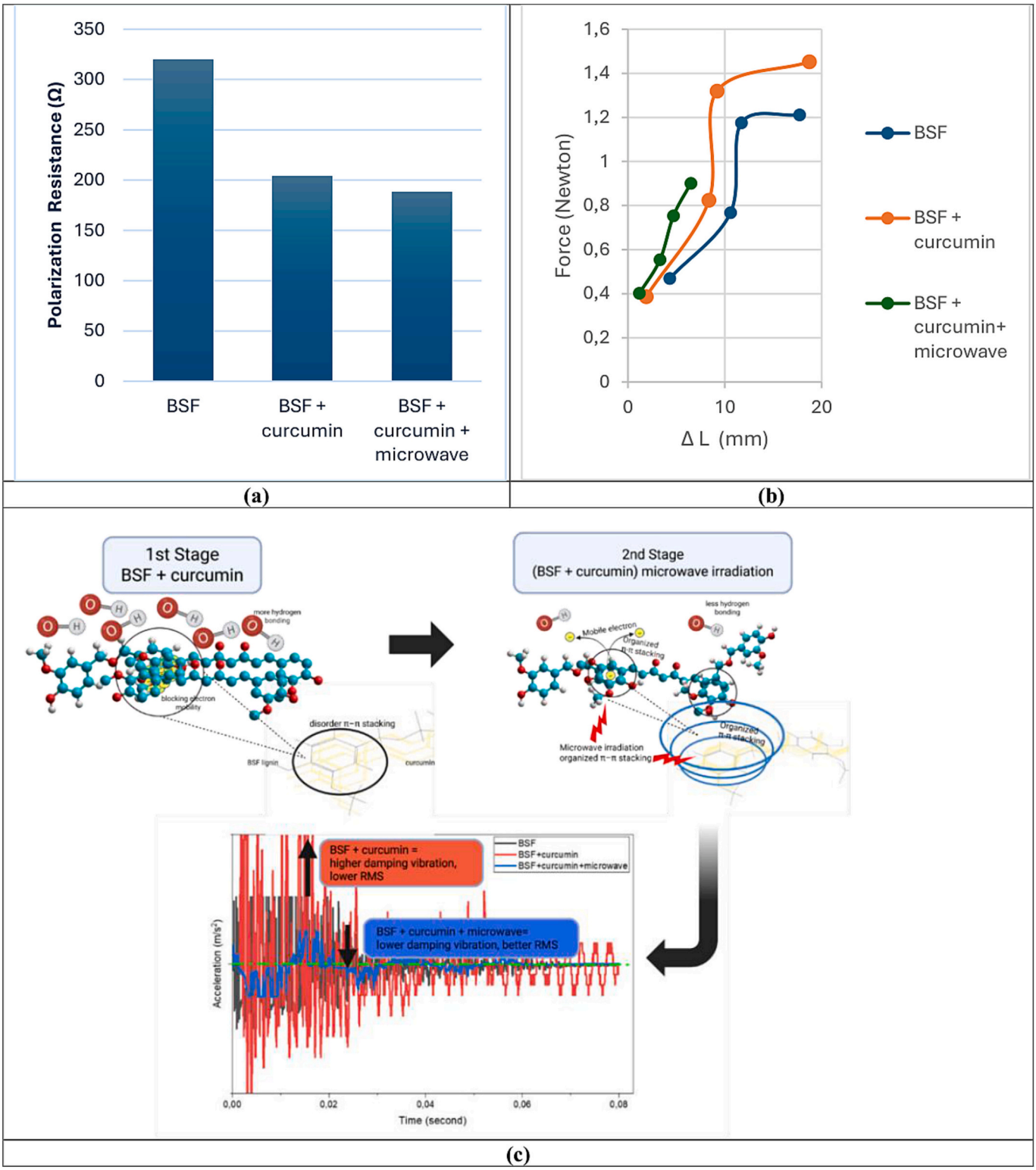

Fig. 5. Electromechanical response and vibrational performance of banana stem fiber (BSF): (a) Polarization resistance showing interfacial polarization changes after curcumin and microwave treatment. (b) Force–deformation response based on quasi-static stiffness tests ($n = 4$). (c) Proposed mechanism illustrating molecular-level contributions to enhanced vibration damping.

Footnote: "Polarization resistance data are shown as single-run results ($n = 1$) for each condition; hence, error bars are not applicable. The corresponding polarization curves for each sample are available in Supplementary Files (Fig. S1).

Table 1
The result of experiment in three variants BSF.

	BSF		BSF + curcumin		BSF + curcumin + microwave	
	Average	Std. dev	Average	Std. dev	Average	Std. dev
Log Decrement (δ)	0.025	± 0.0031	0.308	± 0.030	0.236	± 0.025
Damping Ratio (ζ)	0.004	± 0.0007	0.049	± 0.006	0.038	± 0.005
Root Mean Square (m/s^2)	0.144	± 0.010	0.877	± 0.055	0.087	± 0.008
Stiffness (N/mm)	0.087	± 0.020	0.131	± 0.056	0.222	± 0.100
Strain (ε)	0.091	± 0.047	0.088	± 0.057	0.031	± 0.018

Vibration testing was repeated five times per group ($n = 5$); stiffness measurements were conducted independently with four replicates ($n = 4$). All values are expressed as mean ± standard deviation.

Table 2
ISO 2631 RMS acceleration comfort zones and recommended actions.

RMS acceleration range	Comfort Evaluation	Recommended Action
<0.315	Not uncomfortable	No action needed
0.315–0.63	A little uncomfortable	Caution advice for prolonged exposure
0.63–1.0	Fairly uncomfortable	Reduce exposure time or improve damping
>1.0	Uncomfortable to extremely comfortable	Urgent mitigation recommendation

Source: Adapted from ISO 2631-1:1997 (Evaluation of human exposure to whole-body vibration).

Table 3
Damping ratio (ζ) and RMS acceleration of BSF systems compared with selected reference materials.

Material Type	Damping Ratio (ζ)	RMS Acceleration (m/s^2)	Notes	Source
Flax fiber (natural)	~0.040	Not reported	Moderate damping behavior in dynamic tests	(Nguyen et al., 2024)
Sisal fiber (natural)	~0.045	Not reported	Comparable to flax, good viscoelastic response	(Nguyen et al., 2024)
Coir-polyester composite	~0.050	Not reported	Higher damping than neat polyester	(Şimşir et al., 2024)
Rubber-core sandwich composite	0.18–0.24	0.07	Impact hammer test (beam mode)	(D'Ottavio et al., 2021)
This study (BSF)	0.004	0.144	Untreated banana stem fiber	Present work
This study (BSF + Curcumin)	0.049	0.877	Enhanced damping, low stiffness	Present work
This study (BSF + Curcumin + Microwave)	0.038	0.087	Balanced damping and stiffness	Present work

(Hasan et al., 2022; Romero-Zúñiga et al., 2023).

3.8. General discussion of vibrational damping enhancement

The combined curcumin treatment and microwave activation of banana stem fiber (BSF) induces complementary structural rearrangements that collectively enhance vibrational energy dissipation. A pronounced suppression of vibration acceleration was achieved in the microwave-activated curcumin BSF, with RMS reduced by nearly 39.58% relative to the untreated fiber, as evidenced in Table 1. This improvement was attributed to enhanced molecular alignment, reduced amorphous content, and more efficient intermolecular energy transfer within the modified lignocellulosic network, as supported by the structural trends discussed in the preceding sections.

In untreated and curcumin-only treated fibers, π–π stacking remains irregular, and the high density of hydroxyl groups creates a polar, disordered surface environment, as observed in the FTIR spectra (Fig. 3b). These features restrict charge delocalization and limit the uniform redistribution of vibrational energy, as indicated by Profex-based density maps (Fig. 4a–b). Although curcumin introduces aromatic domains that enable viscoelastic dissipation, it may also increase localized disorder and hydroxyl-related polarity, thereby reducing long-range electron mobility, as reflected by the higher polarization resistance (Fig. 5a), and contributing to elevated RMS acceleration, consistent with the higher strain response (Fig. 5b).

Microwave irradiation initiates a second stage of structural refinement (Romero-Zúñiga et al., 2023)Through dielectric activation, partial dehydration and increased chain mobility are promoted, enabling a selective reduction of hydroxyl-rich environments and improved ordering of aromatic domains (Xu et al., 2024). Consequently, π–π stacking becomes more coherent inferred from the FTIR response (Fig. 3b), interfacial charge transport was enhanced indicated by areas of elevated electron density (Fig. 4c) and by the reduced polarization resistance (Fig. 5a), and modulation of vibrational energy becomes more stable reflected by the proposed mechanistic interpretation (Fig. 5c). The concurrent reduction in peak amplitude and RMS acceleration further suggests strengthened intermolecular interactions and a reinforced internal framework, which is consistent with the increased stiffness response observed after microwave activation (Fig. 5b).

The mechanism illustrated in Fig. 5c describes a two-phase pathway in which microwave irradiation actively reorganizes the atomic and aromatic stacking of curcumin and lignin domains through electromagnetic interactions and charge-mediated responses. Curcumin initially introduces aromatic units into the disordered cellulose microstructure, while subsequent microwave exposure promotes realignment of these domains into a more ordered stacking configuration with improved structural integrity. This rearrangement is supported by the evolution of %T features in the FTIR spectra (Fig. 3b), which indicate reduced hydroxyl dominance and strengthened aromatic interactions, as well as by the decreased polarization resistance reflecting enhanced interfacial charge delocalization (Fig. 5a). In this context, microwave activation mitigates the limitation observed in curcumin-only treated fibers, where increased damping arises from localized viscoelastic loss but remains accompanied by high RMS acceleration due to insufficient structural coherence. The resulting ordered aromatic network enables more uniform redistribution of vibrational energy through improved electron delocalization, consistent with prior reports on interfacial dynamics, molecular orientation, and surface compatibility governing damping behavior in natural fiber systems (Jawaid and Khalil, 2011; Li et al., 2021). Enhanced ordering under microwave exposure also aligns with observations reported for bamboo and hybrid fibers subjected to electromagnetic activation.

Scientifically, the present results indicate that π–π stacking

alignment and hydroxyl group modulation are key molecular-scale contributors to vibrational damping enhancement. The transition from a hydrogen-bond-dominated lignocellulosic system toward a partially conjugated and more crystalline architecture enables a hybrid dissipation pathway that integrates viscoelastic energy loss with charge-assisted energy redistribution. Such a combined mechanism is not typically achieved through conventional natural fiber treatments, thereby underscoring the novelty of the dual curcumin–microwave modification strategy.

From an application perspective, the reduced RMS acceleration and balanced damping characteristics of microwave-activated curcumin BSF support its suitability for vibration-sensitive systems, including automotive seating, ergonomic flooring, industrial mounts, and vehicle interior structures. The mechanistic framework illustrated in Fig. 5c further suggests that the process is scalable and that sequential molecular engineering can be used to tailor both structural coherence and functional vibration performance in sustainable damping materials.

Microwave treatment (900 W for 120 s) plays a dominant role in reorganizing the π–π stacking configuration through dielectric activation governed by energy dissipation, expressed as $P_D = 2\pi f \varepsilon_0 \varepsilon' E_{rms}^2$ (Bagoun et al., 2024). Here, $P_D$denotes the dissipated power per unit volume, $f$is the microwave frequency (2.45 GHz), $\varepsilon_0$is the vacuum permittivity, $\varepsilon'$is the dielectric constant, and $E_{rms}$is the root-mean-square electric field.

The E_{rms}component enhances molecular kinetic energy via dipolar polarization while simultaneously inducing vibrational excitation of curcumin and fiber molecules. This process elevates the temperature from 27.6 ± 0.35 °C to 52.5 ± 0.55 °C, which remains within the thermal stability range of lignin and cellulose (Chandrasekharan Nair et al., 2025). Nevertheless, the temperature increase weakens hydrogen bonding, as evidenced by FTIR spectra (Fig. 3b), thereby facilitating π–π stacking reorganization. This structural rearrangement increases electron density (Fig. 4c) and reduces polarization resistance (Fig. 5a). Collectively, these effects enhance material stiffness, leading to improved vibrational damping and a reduction in RMS amplitude.

Beyond vibration attenuation, the banana stem fiber system also offers environmental advantages compared with conventional synthetic vibration isolation materials. The fibers are derived from agricultural biomass waste and are inherently renewable and biodegradable, reducing end-of-life impact relative to petroleum-based elastomers or polymer foams. Although curcumin treatment and microwave exposure introduce additional processing steps, both rely on food-grade, non-toxic compounds and solvent-free, energy-efficient activation methods commonly used in biomass processing. While a full life cycle assessment is beyond the scope of this study, the proposed modification route represents a lower-toxicity and potentially more sustainable alternative for vibration damping applications.

In summary, the synergistic interaction between curcumin functionalization and microwave-induced aromatic realignment advances a molecular design framework for next-generation natural fiber damping materials. Consistent evidence across structural, electrical, thermal, and dynamic analyses demonstrates that ordered aromatic stacking, reduced polarity, and improved molecular coherence jointly govern enhanced vibrational energy dissipation in the modified banana stem fiber system.

4. Conclusion

This study investigated structural, thermal, and vibrational performance enhancements in banana stem fiber (BSF) achieved through curcumin functionalization followed by microwave activation. Untreated BSF exhibited a hydroxyl-rich, amorphous-dominated structure with limited crystallinity, restricted charge mobility, and only moderate vibration attenuation. Curcumin treatment introduced aromatic and carbonyl functionalities that enhanced viscoelastic dissipation and yielded the highest damping ratio ($\zeta = 0.049 \pm 0.006$). However, the accompanying reduction in thermal stability and the highest RMS acceleration (0.877 ± 0.055 m/s^2) demonstrated that increased cycle-by-cycle energy dissipation did not necessarily translate into improved vibrational comfort, reflecting reduced structural coherence and increased compliance.

Microwave activation produced the most refined material through dielectric-driven reorganization rather than thermal degradation. Under 900 W for 120 s, the temperature increase remained moderate (27.6 ± 0.35 °C to 52.5 ± 0.55 °C), well within the stability range of lignocellulosic components. Integrated FTIR, XRD, Profex, and TGA analyses revealed reduced hydroxyl dominance, enhanced crystallinity, and improved ordering of aromatic domains that promote coherent π–π stacking and more uniform vibrational energy redistribution. These structural refinements were accompanied by reduced polarization resistance (188.26 Ω) and increased stiffness, indicating improved molecular packing and alignment. As a result, the microwave-assisted curcumin-treated BSF achieved the lowest RMS acceleration (0.087 ± 0.008 m/s^2) and suppressed peak vibration, meeting ISO 2631 comfort considerations while maintaining adequate damping capacity and improved thermal resistance.

Overall, the findings demonstrate that vibrational comfort is governed by the coupled effects of damping and stiffness-controlled dynamics rather than damping ratio alone. Microwave-assisted curcumin treatment effectively transforms BSF into a structurally coherent, high-performance bio-based damping material suitable for vibration-sensitive applications such as automotive seating, machinery isolation, ergonomic flooring, and vehicle interior components. Future work should address scale-up feasibility, long-term cyclic durability, and composite integration to further advance industrial applicability.

CRediT authorship contribution statement

Hastawati Chrisna Suroso: Writing – original draft, Visualization, Software, Methodology, Formal analysis. **Eko Siswanto:** Supervision, Conceptualization. **Sugiono:** Supervision, Conceptualization. **I.N.G. Wardana:** Writing – review & editing, Validation, Data curation, Conceptualization.

Funding

This research work received no external funding.

Declaration of competing interest

The authors declare that they have no known competing financial interests or personal relationships that could have appeared to influence the work reported in this paper.

Data availability

Data will be made available on request.

Acknowledgment

The authors gratefully acknowledge the Laboratory of Vibration Engineering and Automotive Systems at Sepuluh Nopember Institute of Technology, the Integrated Research Laboratory at Universitas Brawijaya, and the Laboratory of Analytical and Measurement Services, Department of Chemistry, Faculty of Mathematics and Natural Sciences, Universitas Brawijaya, for their valuable support in providing experimental facilities, technical assistance, and instrumentation throughout the course of this research.

Appendix A. Supplementary data

Supplementary data to this article can be found online at https://doi.

org/10.1016/j.biteb.2026.102644.

References

Abdolmaleki, A., Zare, S., Saghiri, M.A., 2023. Synthesis and characterization of biodegradable poly(ester-imide) nanocomposites with L-alanine, curcumin, and modified <scp>rGO</Scp>. Polym. Adv. Technol. 34 (8), 2674–2683. https://doi.org/10.1002/pat.6081.

Ali, B., Azab, M., Ahmed, H., Kurda, R., El Ouni, M.H., Elhag, A.B., 2022. Investigation of physical, strength, and ductility characteristics of concrete reinforced with banana (*Musaceae*) stem fiber. J. Build. Eng. 61. https://doi.org/10.1016/j.jobe.2022.105024.

Almutairi, F.M., El-Ghoul, Y., Jabli, M., 2021. Extraction of cellulose polymeric material from populus tremula fibers: characterization and application to the adsorption of methylene blue and crystal violet. Polymers 13 (19), 3334. https://doi.org/10.3390/polym13193334.

Bagoun, R., EL Khouakhi, M., Chaouki, J., Lhoussaine, O., EL Asri, M., 2024. Optimizing phosphoric acid concentrating using microwave technology: theoretical and empirical model of energy efficiency and P2O5 concentration. Chem. Eng. Process. Process Intensif. 203. https://doi.org/10.1016/j.cep.2024.109882.

Barros, L.N.L.C., Araujo, R.N., Nascimento, E.P.d., Gama, A., Neves, G.d.A., Morales, M. A., Menezes, R.R., 2024. Influence of fast drying on the morphology of A-Fe2O3 and FeMnO3/α-Fe2O3 fibers produced by solution blow spinning. Nanomaterials 14 (3), 304. https://doi.org/10.3390/nano14030304.

Chandrasekharan Nair, S., John, V., Geetha Bai, R., Kikas, T., 2025. Torrefaction of lignocellulosic biomass: a pathway to renewable energy, circular economy, and sustainable agriculture. In: Sustainability (Switzerland), Vol. 17, Number 17. Multidisciplinary Digital Publishing Institute (MDPI). https://doi.org/10.3390/su17177738.

Dhanenderan, N., Uvaraja, V.C., Raj, J.B., Malarkodi, P., 2022. Physical, chemical and thermal analysis of banana flower pistil fiber for the potential application of composite manufacturing. Proc. Inst. Mech. Eng. Part E J. Process Mech. Eng. 237 (4), 1344–1353. https://doi.org/10.1177/09544089221113410.

Dong, M., Cao, C., Luo, Z., Ni, S., Bian, H., Dai, H., Gao, Y., 2025. Lignin nanoparticles-engineered cellulose nanofibrils films with modulated surface microstructure and interfacial polarization for high-performance triboelectric nanogenerators. Chem. Eng. J. 524. https://doi.org/10.1016/j.cej.2025.169234.

D'Ottavio, M., Krasnobrizha, A., Valot, E., Polit, O., Vescovini, R., Dozio, L., 2021. Dynamic response of viscoelastic multiple-core sandwich structures. J. Sound Vib. 491. https://doi.org/10.1016/j.jsv.2020.115753.

Drouiche, F., Laouici, H., Cheikh, M., 2023. Morphological, chemical, thermal and mechanical analysis of doum fibers as potential reinforcement of polymer composites. J. Compos. Mater. 58 (1), 37–54. https://doi.org/10.1177/00219983231215418.

Ethaib, S., 2024. Microwave-assisted pretreatment for lignocellulosic biomass energy conversion path. In: Bioresource Technology Reports, Vol. 28. Elsevier Ltd. https://doi.org/10.1016/j.biteb.2024.102006.

Gupta, U.S., Dhamarikar, M., Dharkar, A., Chaturvedi, S., Tiwari, S., Namdeo, R., 2020. Surface modification of banana fiber: a review. Mater. Today Proc. 43, 904–915. https://doi.org/10.1016/j.matpr.2020.07.217.

Guruguntla, V., Lal, M., 2022. Multi-body modelling and ride comfort analysis of a seated occupant under whole-body vibration. J. Vib. Control. 29 (13–14), 3078–3095. https://doi.org/10.1177/10775463221091089.

Hasan, A., Rabbi, M.S., Maruf Billah, M., 2022. Making the lignocellulosic fibers chemically compatible for composite: a comprehensive review. In: Cleaner Materials, Vol. 4. Elsevier Ltd. https://doi.org/10.1016/j.clema.2022.100078.

Hidalgo-Salazar, M.A., Correa-Aguirre, J.P., Román, A.J., González, R., Vera, R.E., Osswald, T.A., 2024. Colombian natural fibers: potential applications in sustainable natural fiber reinforced composites materials. Polym. Compos. 46 (6), 5599–5617. https://doi.org/10.1002/pc.29313.

de la Hoz-Torres, M.L., Aguilar, A.J., Ruíz, D.P., Martínez-Aires, M.D., 2022. Whole body vibration exposure transmitted to drivers of heavy equipment vehicles: a comparative case according to the short- and long-term exposure assessment methodologies defined in ISO 2631-1 and ISO 2631-5. Int. J. Environ. Res. Public Health 19 (9), 5206. https://doi.org/10.3390/ijerph19095206.

Jawaid, M., Khalil, H.P.S.A., 2011. Cellulosic/synthetic fibre reinforced polymer composites: a review. Carbohydr. Polym. 86 (1), 1–18. https://doi.org/10.1016/j.carbpol.2011.04.043.

Kustanto, Sonief, A.A.A., Hamidi, N., Wardana, I.N.G., 2024. Increasing thermal energy absorption in single RGO/curcumin/C60 molecules using microwave induction. Case Stud. Chem. Environ. Eng. 10. https://doi.org/10.1016/j.cscee.2024.100899.

Li, Guo-Ling, Zhuo, Z., Wang, B., Cao, X., Su, H., Wang, W., Huang, Y., Hong, M., 2021. Constructing Π-stacked supramolecular cage based hierarchical self-assemblies via Π···π stacking and hydrogen bonding. J. Am. Chem. Soc. 143 (29), 10920–10929. https://doi.org/10.1021/jacs.1c01161.

Mansingh, B.B., Binoj, J.S., Siengchin, S., Rangappa, S.M., 2022. Influence of surface treatment on properties of *Cocos Nucifera* L. var typica fiber reinforced polymer composites. J. Appl. Polym. Sci. 140 (3). https://doi.org/10.1002/app.53345.

Moghaddam, A.H., Maboudi, K., Bavaghar, B., Sangdehi, S.R.M., Zare, M., 2021. Neuroprotective effects of curcumin-loaded nanophytosome on ketamine-induced schizophrenia-like behaviors and oxidative damage in male mice. Neurosci. Lett. 765. https://doi.org/10.1016/j.neulet.2021.136249.

Nguyen, A.V., Charlet, K., Bouzgarrou, B.C., Pham, K.N., Béakou, A., 2024. Damping analysis of natural fibers and natural fibers reinforced composite. In: Mo, J.P.T. (Ed.), Proceedings of the 10th International Conference on Mechanical, Automotive and Materials Engineering. Springer Nature Singapore, pp. 295–302.

Omoriyekomwan, J.E., Tahmasebi, A., Zhang, J., Yu, J., 2022. Synthesis of super-long carbon nanotubes from cellulosic biomass under microwave radiation. Nanomaterials 12 (5), 737. https://doi.org/10.3390/nano12050737.

Patty, P.J., Wattimena, S.C., 2023. Crystalline properties of cassava (Manihot Esculenta Crantz) starch and its associated biofoam. Jurnal Fisika Dan Aplikasinya 19 (2), 49. https://doi.org/10.12962/j24604682.v19i2.16576.

Ponce-Ruiz, J.L.A., Ishizuka, S., Todaka, Y., Yamada, Y., Reyes-Serrato, A., Ramírez, J.M. H., 2022. Theoretical and experimental study of CaMgSi thermoelectric properties. ACS Omega 7 (18), 15451–15458. https://doi.org/10.1021/acsomega.1c07307.

Qian, S., Wang, J., Liu, Z., Mao, J., Zhao, B., Mao, X., Zhang, L., Cheng, L., Zhang, Y., Sun, X., Cui, W., 2022. Secretory fluid-aggregated janus electrospun short fiber scaffold for wound healing. Small 18 (36). https://doi.org/10.1002/smll.202200799.

Romero-Zúñiga, G.Y., Sánchez-Valdés, S., Ceniceros-Reyes, M.A., Sifuentes-Nieves, I., Gallardo-Vega, C.A., Solís-Rosales, S.G., González-Morones, P., Hernández-Hernández, E., 2023. A one-step process to produce high-crystallinity cellulose microfibrils from microwave irradiation of natural fiber waste. Cellulose 30 (16), 10067–10082. https://doi.org/10.1007/s10570-023-05493-1.

Sakib, S.N., Payne, D.N., Kim, J., Huang, S., Puthen-Veettil, B., 2024. Rapid microwave annealing for improved crystallinity and morphology of perovskite materials. Sol. RRL 8 (24). https://doi.org/10.1002/solr.202400585.

Sánchez-Martín, M.d.M., Giraldo, E., Roca, F.G., Alastrue-Agudo, A., Martínez-Ramos, C., Pradas, M.M., Moreno-Manzano, V., 2023. Acute transplantation of NPC on electrospun poly-lactic acid membranes containing curcumin into the injured spinal cord reduces neuronal degeneration. Front. Biomater. Sci. 2. https://doi.org/10.3389/fbiom.2023.1298894.

Schirp, A., Deetz, R., Kopitzky, R., Schirp, C., 2024. Composite sheets based on polylactic acid and sugar beet pulp: a solution to accelerate biological degradation of <scp>PLA</Scp> on Soil under outdoor exposure. Polym. Compos. 45 (16), 15318–15339. https://doi.org/10.1002/pc.28840.

Silva, D.J.d., Souza, A.G., Camani, P.H., Rosa, D.d.S., 2023. Bactericidal properties of natural fibers hybrid functionalized with ZnO/Cu2+ and ZnO/Cu0. Fibers Polym. 24 (3), 959–973. https://doi.org/10.1007/s12221-023-00030-0.

Şimşir, E., Akçin Ergün, Y., Yavuz, İ., 2024. Investigation of damping properties of natural fiber-reinforced composites at various impact energy levels. Polymers 16 (24). https://doi.org/10.3390/polym16243553.

Singh, R.P., Nayak, S.K., Hegde, S., Padmaraj, N.H., 2023. Influence of fiber length and moisture content on sound and vibration characteristics of hemp/epoxy composites. Istrazivanja I Projektovanja Za Privredu 21 (3), 957–962. https://doi.org/10.5937/jaes0-44872.

Smalley, C.J.H., Hughes, C.E., Hildebrand, M., Aizen, R., Bauer, M., Yamano, A., Levy, D., Mirsky, S.K., Shaked, N.T., Young, M.T., Kolb, U., Gazit, E., Kronik, L., Harris, K.D.M., 2024. Understanding the solid-state structure of riboflavin through a multitechnique approach. Cryst. Growth Des. 24 (15), 6256–6266. https://doi.org/10.1021/acs.cgd.4c00480.

Sobri, S., Wijayanti, W., Hamidi, N., Purnami, Nugroho, W.S., Wardana, I.N.G., 2025. Engineered seabed sediment via microwave-assisted Ni^{2+} substitution as a catalyst for double-stage pyrolysis of plastic waste: a novel approach to methane reforming and enhanced hydrogen production. Results Eng. 27. https://doi.org/10.1016/j.rineng.2025.106488.

Thimmegowda, D.Y., Hindi, J., Markunti, G.B., Kakunje, M., 2025. Enhancement of mechanical properties of natural fiber reinforced polymer composites using different approaches—a review. J. Compos. Sci. 9 (5). https://doi.org/10.3390/jcs9050220. Multidisciplinary Digital Publishing Institute (MDPI).

Tu, W.C., Hallett, J.P., 2019. Recent advances in the pretreatment of lignocellulosic biomass. Curr. Opin. Green Sustain. Chem. 20, 11–17. Elsevier B.V. https://doi.org/10.1016/j.cogsc.2019.07.004.

Wang, Q., Liu, S., Lu, W., Zhang, P., 2022. Fabrication of Curcumin@Ag loaded core/shell nanofiber membrane and its synergistic antibacterial properties. Front. Chem. 10. https://doi.org/10.3389/fchem.2022.870666.

Wang, L., Jiang, X., Zhao, C., Chen, Y., Chen, C., Tu, N., Nie, X., Gao, Q., Zhang, W., Zhang, Y., Zhao, N., Li, Z., Huang, X., 2025. Critical role of interfacial polarization suppression in enhancing breakdown strength and energy storage performance of NBT-based dielectric ceramics. J. Mater. Chem. A 13 (35), 29368–29378. https://doi.org/10.1039/D5TA04485E.

Xu, K., Zheng, Y., Zhou, J., Zhao, Y., Pang, X., Cheng, L., Wang, H., Zhang, X., Zhang, R., Jiang, Z., 2024. Microwave-assisted fabrication of highly crystalline, robust COF membrane for organic solvent nanofiltration. Adv. Funct. Mater. 35 (12). https://doi.org/10.1002/adfm.202417383.

Yu, Y., Song, X., Wang, Y., Lai, R.P., Nie, Y., Xiang, W., Zhou, C., Zhao, S., Liu, H., 2025. Defect-mediated permeation of deep eutectic solvents in cellulose crystals: a combined experimental and molecular dynamics study. Carbohydr. Polym. 369. https://doi.org/10.1016/j.carbpol.2025.124331.

Zhan, L., Pei, J., Yuan, J., Li, Y., Ji, F., Wang, N., 2023. Novel nano $BaTiO_3$-based microwave vacuum treatment for precise and controllable scales stripping of wool fibers. Text. Res. J. 93 (11−12), 2708–2717. https://doi.org/10.1177/00405175221147726.

Zhang, W., He, C., 2022. Investigation and prediction of mechanical properties of hot water treated jute/poly(lactic acid) composite laminates using response surface

methodology and genetic algorithm. Polym. Compos. 43 (10), 7170–7186. https://doi.org/10.1002/pc.26780.

Zhang, Yingchuan, Xu, F., Chen, F., Zhang, Yanru, Wu, Y., Jiang, L., 2022. Dual utilization of lignocellulose biomass and glycerol waste to produce fermentable levoglucosan via fast pyrolysis. Front. Chem. 10. https://doi.org/10.3389/fchem.2022.847767.

Zhao, X., Schindler, C., 2014. Evaluation of whole-body vibration exposure experienced by operators of a compact wheel loader according to ISO 2631-1:1997 and ISO 2631-5:2004. Int. J. Ind. Ergon. 44 (6), 840–850. https://doi.org/10.1016/j.ergon.2014.09.006.